Effect of a frictional force on the Fermi–Ulam model

2006 J. Phys. A: Math. Gen. 39 11399

(http://iopscience.iop.org/0305-4470/39/37/005)

INSTITUTE OF PHYSICS PUBLISHING JOURNAL OF PHYSICS A: MATHEMATICAL AND GENERAL

J. Phys. A: Math. Gen. **39** (2006) 11399–11415 doi:10.1088/0305-4470/39/37/005

Effect of a frictional force on the Fermi–Ulam model

Edson D Leonel[1] **and P V E McClintock**[2]

[1] Departamento de Estatística, Matemática Aplicada e Computação, Instituto de Geociências e Ciências Exatas, Universidade Estadual Paulista, UNESP, Av. 24A, 1515 Bela Vista, 13506-700 Rio Claro, SP, Brazil
[2] Department of Physics, Lancaster University, Lancaster, LA1 4YB, UK

Received 27 May 2006, in final form 21 July 2006
Published 29 August 2006
Online at stacks.iop.org/JPhysA/39/11399

Abstract

The dynamical properties of a classical particle bouncing between two rigid walls, in the presence of a drag force, are studied for the case where one wall is fixed and the other one moves periodically in time. The system is described in terms of a two-dimensional nonlinear map obtained by solution of the relevant differential equations. It is shown that the structure of the KAM curves and the chaotic sea is destroyed as the drag force is introduced. At high energy, the velocity of the particle decreases linearly with increasing iteration number, but with a small superimposed sinusoidal modulation. If the motion passes near enough to a fixed point, the particle approaches it exponentially as the iteration number evolves, with a speed of approach that depends on the strength of the drag force. For a simplified version of the model it is shown that, at low energies corresponding to the region of the chaotic sea in the non-dissipative model, the particle wanders in a chaotic transient that depends on the strength of the drag coefficient. However, the KAM islands survive in the presence of dissipation. It is confirmed that the fixed points and periodic orbits go over smoothly into the orbits of the well-known (non-dissipative) Fermi–Ulam model as the drag force goes to zero.

PACS numbers: 05.54.−a, 05.45.Ac, 05.45.Pq

(Some figures in this article are in colour only in the electronic version)

1. Introduction

A class of one-dimensional time-dependent systems that has been exhaustively investigated in recent years is that related to the so-called one-dimensional Fermi accelerator model. The latter was originally proposed by Fermi [1] in order to describe the acceleration of cosmic rays. It provides a mechanism through which charged particles can be accelerated by collisions with time-dependent magnetic fields. The model was subsequently studied in different versions and using a number of different approaches [2–6]. One of them, known as the Fermi–Ulam model

(FUM), considers the dynamics of a classical particle bouncing between two rigid walls, one of which is fixed and the other moves in time. The main result for periodic oscillation is that the phase space presents Kolmogorov–Arnol'd–Moser (KAM) islands surrounded by a chaotic sea. Unlimited energy growth (i.e., the needed condition for observing Fermi acceleration) is not, however, observed because the phase space exhibits a set of invariant spanning curves [7]. An alternative version of this model proposed by Pustylnikov [8], often referred to as a bouncer, consists of a classical particle falling in a constant gravitational field, on a moving platform. Its most important property is that, in contradistinction to the FUM, depending on both the initial conditions and control parameters, there is no bound on the energy gained by the bouncing particle. This special difference between the models was later clarified by Lichtenberg, Lieberman and Cohen [9]. We have recently proposed [10] a hybrid version of the Fermi–Ulam accelerator and bouncer models. The system behaves not exclusively as pure Fermi–Ulam nor as a pure bouncer model, but as a combination of the two. We used a simplified version of the model to obtain analytically the conditions for which properties that are individually present in the Fermi–Ulam (high energy invariant spanning curves) and bouncer models (low energy invariant spanning curves) but that come out and coalesce together in the hybrid version of the model. The corresponding quantum versions of both the bouncer model and FUM have also been studied [11–15].

The special interest attached to studying these one-dimensional classical systems is that they are completely integrable for zero external time-dependent forcing, but non-integrable when the external forcing is switched on. Furthermore, they allow direct comparison of theoretical predictions with experimental results [16–18]. Such systems present a very rich phase space structure. Depending on the values of the control parameters, as well as on the initial conditions, periodic, quasi-periodic and chaotic behaviour all can be observed. This mixed phase space structure has also been observed for one-dimensional time-dependent potentials [19–24] and for billiards with static boundaries [25–28], and is indeed generic for non-degenerate Hamiltonian systems. When time-dependent boundaries are considered for such billiards, however, the scenario that arises is quite different. One of the main questions addressed in studies of such problems is how the energy of the particle varies with time and, in particular, whether or not the system can exhibit the phenomenon of Fermi acceleration. A discussion of these very interesting questions, together with specific examples, can be found in [29] where the authors conjectured that: 'Chaotic dynamics of a billiard with a fixed boundary is a sufficient condition for Fermi acceleration in the system when a boundary perturbation is introduced'. Recently, the well-known annular billiard has been investigated [30, 31] to try and verify this conjecture and to enlarge the number of cases to which it is applicable.

It is also interesting to investigate the effects of dissipation in these systems. Different kinds of perturbation can be introduced including: (i) a loss of energy at each impact, through inelastic collisions with the moving wall or (ii) the effect of a frictional (drag) force. For the bouncer model, with the dissipation introduced via inelastic collisions, a variety of interesting results were found [32–35], while the version with a frictional force was carefully analysed in [36, 37]. For the FUM with inelastic collisions, remarkable effects of the dissipation on its dynamics and other properties were discussed [38–40] and, in particular, crisis events were observed and characterized [41]. A more complex case consisting of a combination of the FUM with a half-stadium was discussed [42]. However, an important question that, to our knowledge, has not yet been addressed relates to what happens with the asymptotic behaviour of individual initial conditions to the FUM when—as is so often the case in practice—a frictional force is present. This seems to be a lacuna for both the complete and simplified versions of the FUM.

In this paper, we study a dissipative version of the FUM. It consists of a classical particle bouncing between two rigid walls in the presence of a drag force. As usual, we suppose one wall to be fixed and the other to move periodically in time. We characterize the dynamics of this system by using a two-dimensional nonlinear map, and we consider it in two different versions: (i) complete and (ii) simplified. The map is obtained via the solution of differential equations. We will show that, under the perturbation of the drag force, the dynamics of this system becomes very different from that of the non-dissipative case and that, furthermore, the nature of the differences varies depending on the region considered. In the high energy domain of both versions, where it is well known that invariant spanning curves exist in the non-dissipative case, the velocity of the particle decreases linearly with increasing iteration number. In the low energy domain, within the region corresponding to the chaotic sea for the non-dissipative case, the particle experiences a chaotic transient that depends on the magnitude of the drag force coefficient. For these regions, the asymptotic behaviour of the particle is to come to rest. Thus, the drag force dissipates all of the particle's initial energy. We will find, however, that the dynamics of the particle near fixed points differs markedly between the two versions of the model. For the complete version, the particle approaches the fixed point exponentially as the iteration number evolves, at a rate depending on the strength of the drag coefficient. In the simplified version, however, the KAM islands survive the perturbation. In particular, we will show that the fixed points and the corresponding map go over smoothly to the fixed points and map of the non-dissipative FUM. A short letter reporting the observation of area preservation within the simplified FUM has already been published [43].

This paper is organized as follows. In section 2, we provide all details needed to construct the map describing the dynamics of the complete version and we discuss the numerical results obtained from it. Section 3 describes some properties of the simplified version, presents a connection with the non-dissipative FUM and also reports the numerical results. Finally, we summarize and draw conclusions in section 4.

2. Map derivation for the complete version of the FUM under a frictional force

The model thus consists of a classical particle of mass m, confined between and bouncing elastically between a wall fixed at $x = l$ and a wall moving periodically in time according to the equation $x_{\mathrm{w}}(t) = \varepsilon\cos(\omega t)$. The parameter ε is the amplitude of oscillation while ω denotes the angular frequency. The particle experiences a drag force, equivalent to being immersed in a fluid of viscosity η', e.g. a gas, that we suppose to be unaffected by the motion of the moving wall. The dynamics of this model is described via a map T that gives the velocity of the particle immediately after a collision with the moving wall as well as the time of that collision, i.e. $(v_{n+1}, t_{n+1}) = T(v_n, t_n)$. Before starting to construct the map, we first discuss the initial conditions. We suppose that at a time $t = t_n$ and after suffering a collision with the moving wall the particle has initial velocity $v = v_n$ and its position is given by $x_{\mathrm{p}}(t_n) = \varepsilon\cos(\omega t_n)$. The velocity and position of the particle are completely specified by the solution of Newton's second law $\sum F = ma$. In this case, we assume that $\sum F = -\eta' v$ where $a = \mathrm{d}v/\mathrm{d}t$ is the acceleration. The differential equation that must be solved is therefore

$$-\eta' v = m\frac{\mathrm{d}v}{\mathrm{d}t}. \tag{1}$$

We recommend the interested reader who want to follow all the steps of the mapping derivation to look at appendix A. Using dimensionless and more convenient variables, we define $V_n = v_n/(\omega l)$, $\delta = \eta/\omega$, $\epsilon = \varepsilon/l$, where $\eta = \eta'/m$, and also measure time in terms of the number of oscillations of the moving wall, i.e. $\phi_n = \omega t_n$. Using these variables, the

mapping for the general case may then be rewritten as

$$T : \begin{cases} V_{n+1} = V_n^* \, \mathrm{e}^{-\delta\phi_c} - 2\epsilon \sin(\phi_{n+1}) \\ \phi_{n+1} = \phi_n + \Delta T_n \mod 2\pi, \end{cases} \tag{2}$$

where V_n^* and ΔT_n are given by different expressions according to the following conditions:

(1) *Multiple collision.* In this case, $\Delta T_n = \phi_c$ and $V_n^* = -V_n$. The term ϕ_c is obtained as the smallest solution of the function $G(\phi_c)$ in the interval $\phi_c \in (0, 2\pi]$, given by

$$G(\phi_c) = \epsilon \cos(\phi_n + \phi_c) - \epsilon \cos(\phi_n) + \frac{V_n^*}{\delta}(1 - \mathrm{e}^{-\delta\phi_c}). \tag{3}$$

(2) *Single collision.* For this case, we have that $\Delta T_n = \phi_T + \phi_c$ and $V_n^* = V_n - 2\delta + \delta\epsilon(1 + \cos(\phi_n))$. The term ϕ_T is given by

$$\phi_T = -\frac{1}{\delta} \ln\left[1 - \frac{\delta}{V_n}[2 - \epsilon - \epsilon\cos(\phi_n)]\right],$$

while the term ϕ_c is obtained as the smallest solution of the function $F(\phi_c)$ in the interval $\phi_c \in [0, 2\pi]$, given by

$$F(\phi_c) = \epsilon \cos(\phi_n + \phi_T + \phi_c) - \epsilon + \frac{V_n^*}{\delta}(1 - \mathrm{e}^{-\delta\phi_c}). \tag{4}$$

As a consequence of the drag force, the expression for the Jacobian matrix differs from that in the non-dissipative version. After some algebra, it is possible to show

- that for the multiple collisions (case (1)), we have

$$\det J_{\mathrm{cv}} = \mathrm{e}^{-\delta\phi_c}\left[\frac{V_n + \epsilon\sin(\phi_n)}{V_{n+1} + \epsilon\sin(\phi_{n+1})}\right], \tag{5}$$

- and that, for case (2),

$$\det J_{\mathrm{cv}} = \mathrm{e}^{-\delta\phi_c}\left[\frac{V_n + \epsilon\sin(\phi_n)}{V_{n+1} + \epsilon\sin(\phi_{n+1})}\right]\left[1 - \frac{\delta}{V_n}[2 - \epsilon - \epsilon\cos(\phi_n)]\right]. \tag{6}$$

The index 'cv' denotes the complete version. It is interesting to emphasize that in the conservative case the determinant of the Jacobian matrix is $\det J = (V_n + \epsilon\sin(\phi_n))/(V_{n+1} + \epsilon\sin(\phi_{n+1}))$, as can be seen in [10, 44]. Moreover, we can immediately see that equations (5) and (6) both imply a contracting area in the phase space. It is also easy to see, however, that in the limit $\delta \to 0$ for the drag coefficient, equations (5) and (6) both lead to recovery of the result of the FUM. For that limit of δ, it can also be considered as a particular case of the breathing circle in which a particle is bouncing in diametrical orbits [45].

2.1. Numerical results for the complete version of the problem

We discuss in this section our numerical results for the complete version of the problem. Since the mapping is area contracting, it is thus to be expected that, as time evolves and the drag force dissipates the energy of the particle, either of two different things may occur: (i) the particle may be 'captured' by an attracting region (fixed point) related to the corresponding KAM islands in the non-dissipative case, and then approaches the fixed point asymptotically. Such capture depends on how close the particle passes to the attracting region or (ii) the drag force dissipates all the energy of the particle, bringing it to rest. Before discussing the behaviour of the velocity as a function of iteration number, we first investigate it analytically. For high velocity, $V \gg 2\epsilon$ and $\delta \ll \epsilon$, so that we can rewrite expression (2) for the velocity as

$$V_{n+1} \cong V_n - 2\delta - 2\epsilon\sin(\phi_{n+1}), \tag{7}$$

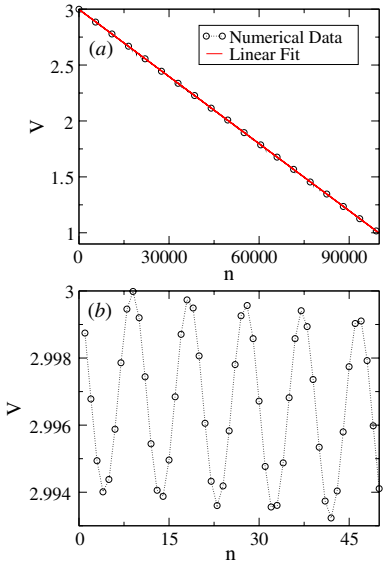

Figure 1. Velocity V as a function of n for the complete version of the FUM under a frictional force. The control parameters used were $\epsilon = 1 \times 10^{-3}$ and $\delta = 1 \times 10^{-5}$. The initial conditions were $V_0 = 3$ and $\phi_0 = 0$. Part (b) is plotted on expanded scales to illustrate the oscillatory behaviour.

where we have considered the product $\delta\epsilon$ to be negligible. Extending this approximation to the exponential, we note that the maximum value of ϕ_c is $\phi_c = 2\epsilon/V_n$. In the limit of $V \gg 2\epsilon$ and $\delta \ll \epsilon$, the expression $e^{-\delta\phi_c} \to 1$. We can then rewrite the iterated equation (7) as

$$V_1 = V_0 - 2\epsilon \sin(\phi_1) - 2\delta$$
$$V_2 = V_0 - 2\epsilon[\sin(\phi_1) + \sin(\phi_2)] - 4\delta$$
$$V_3 = V_0 - 2\epsilon[\sin(\phi_1) + \sin(\phi_2) + \sin(\phi_3)] - 6\delta$$

and then the general expression as

$$V_n = V_0 - 2\epsilon \sum_{i=1}^{n} \sin\phi_i - 2n\delta. \tag{8}$$

Equation (8) tells us that the velocity of the particle decreases linearly as the iteration number increases. However, even supposing that ϕ were uniformly distributed in $\phi \in [0, 2\pi)$, so that the condition yielded $2\epsilon \sum_i \sin\phi_i = 0$, we would still expect the velocity to oscillate sinusoidally for a short range of collision with the moving wall, 'n', as the velocity decreases. Such an oscillation is clearly evident in figure 1 (see part (b)) which plots the calculated velocity as a function of n with the control parameters $\epsilon = 1 \times 10^{-3}$, $\delta = 1 \times 10^{-5}$, for the initial condition $V_0 = 3$ and $\phi_0 = 0$. Figure 1(a) shows that the linear decrease in velocity persists over a large range of n, and figure 1(b) shows the oscillatory velocity on an expanded ordinate scale for a short range of n. A linear fit gives us a linear coefficient of -2×10^{-5}, which is in complete accord with equation (8). It is interesting to emphasize that, when the drag coefficient $\delta \to 0$, the last term in equation (8) disappears. The invariant spanning curves then become stable and the velocity of the particle does not decrease as the dynamics evolves. Moreover, this result is in fact in perfect agreement with that obtained from the determinant

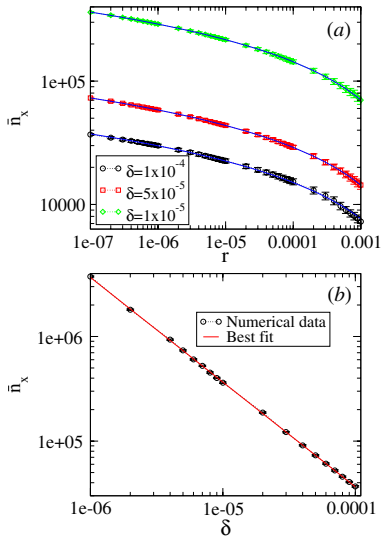

Figure 2. (*a*) Behaviour of the average $\bar{n}_x$ as a function of proximity to the attracting fixed point for the complete version of the dissipative model, as trajectories converge to it. (*b*) The transient $\bar{n}_x$ as a function of the drag coefficient δ.

of the Jacobian matrix in the limit $\delta \to 0$. In this limit, we have the condition of phase space measure preservation and thus the results for the non-dissipative FUM are all recovered.

Now suppose that the particle is captured by an attracting region. We will describe how it approaches the attracting fixed point as a function of iteration number. We shall consider the attracting region as being in some sense equivalent to the first KAM island for the non-dissipative model (cf table 1 for the non-dissipative simplified model and figure 4 for its dissipative version) although other regions could also be considered. In order to investigate the asymptotic approach to the attracting fixed point, we first define a set of initial conditions and then allow the system to evolve in time. We establish a convergency criterion in order to define the asymptotic approach to the attracting fixed point. The criterion consists in checking the distance of the particle from the fixed point. We thus define a circle of radius $r_c = 10^{-6}$ and iterate each set of initial condition. If the particle is near enough to the fixed point, say less than r_c, we then save, in an array, the corresponding number of collisions spent until that point and thus start a different initial condition. After evolving from an ensemble of M different initial conditions, the average $\bar{n}_x$ is given by $\bar{n}_x = 1/M \sum_{i=1}^{M} n_i$.

Using a set of close initial conditions we can characterize the deviations of the computational data. Figure 2(*a*) shows the behaviour of the average number of collisions with the moving wall, $\bar{n}_x$ as a function of proximity to the fixed point for a set of trajectories approaching it. The horizontal axis represents how far the trajectory is from the fixed point, a distance defined as $r = \sqrt{(V_n - V^*)^2 + (\phi_n - \phi^*)^2}$. The coordinates of the fixed point are represented by (V^*, ϕ^*). The error bars denote the standard deviation of a set of 500 different initial conditions in the range $(V_0, \phi_0) = ([0.325, 0.33], \pi)$. Each curve in figure 2(*a*) is fitted by the function $\bar{n}_x(r) = A + B \ln(r)$. For $\delta = 1 \times 10^{-4}$, we obtain $A = -14.6(1) \times 10^3$ and $B = -3.22(1) \times 10^3$. For the case where $\delta = 5 \times 10^{-4}$ we have $A = -29.72(2) \times 10^3$, $B = -6.376(2) \times 10^3$ and finally, for $\delta = 1 \times 10^{-5}$, the coefficients are $A = -149.1(3) \times 10^3$ and $B = -31.77(3) \times 10^3$. Results like those in figure 2(*a*) allow us to conclude that the

trajectory approaches the fixed point exponentially as the collisions with the moving wall evolve. We can also investigate how the trajectory evolves towards an attracting fixed point as a function of the drag coefficient. Figure 2(*b*) shows the behaviour of $\bar{n}_x$ as a function of the drag coefficient where we have evolved the simulation up to $r < 10^{-6}$. We can then describe such behaviour as

$$\bar{n}_x \propto \delta^{\mu}. \tag{9}$$

After doing a power-law fit as those shown in figure 2(*b*) we obtain $\mu = -1.000(2)$. It is easy to see that, in the limit $\delta \to 0$, equation (9) gives us that $\bar{n}_x \to \infty$. Note however that, in this limit of δ, the preservation of the phase space measure must be recovered. We conclude that two different things can occur, depending on the initial conditions: (i) the particle may display periodic, or at least quasi-periodic, behaviour or (ii) the particle may exhibit chaotic behaviour. The result $\bar{n}_x \to \infty$ could be interpreted as indicating that convergence to an attracting fixed point does not occur.

3. A simplified version of the dissipative FUM

Next, we describe a modified form of our dissipative FUM that we refer to as its *simplified version*[3]. We will suppose that both walls are fixed but that, after the particle suffers a collision with one of them, it exchanges momentum as if the wall was moving. Simplifications of this kind were found very useful for speeding up numerical simulations two or three decades ago, when computers were far slower. Such an approach is also useful in facilitating the analytic treatment. It also enables us to seek generic behaviour that can subsequently be sought in the complete version of the model.

Several recent works have used such simplifications to describe the dynamical properties of two-dimensional maps. For example, scaling arguments have been used [46] to characterize the chaotic sea at low energy for the simplified FUM. One of the tools employed in investigating the model, the roughness, was derived from surface science [47] and the formalism proposed in [46] could usefully be applied to billiards (see also [48, 49] for recent results in the simplified Fermi–Ulam model). In [44], the authors used the simplified version of the FUM to provide a careful description of the lowest energy invariant spanning curve and its location. The results are in principle extendable to the complete version of the model. Furthermore, we have used a similarly simplified version of the hybrid Fermi–Ulam-bouncer model [10] to predict the existence of invariant spanning curves below the chaotic sea in the low energy region. We were subsequently able to use the corresponding complete version for observing such curves. The hybrid model in question behaves neither purely as a FUM, nor as a bouncer, but as a combination of these two. Simplifications of this kind have also been found useful in relation to the problem of rippled channels [50–52].

For the non-dissipative case, the complete and simplified versions closely present similar results except at very low energies, typically $V \cong 2\epsilon$. In this limit, it is possible to observe in the complete model a set of successive collisions that are absent in the simplified version. As we will discuss, the introduction of this simplification into our dissipative model yields significantly different asymptotic behaviour for the region related to the fixed points. If we then consider that both walls are fixed, we immediately see that successive collisions that are allowed in the complete model cannot occur in the simplified one. In the complete model, depending on the combination of velocity and phase, it is possible for the particle, after suffering a collision with the moving wall, to suffer a second successive collision before

[3] The simplified FUM was introduced by Lichtenberg and Lieberman and can be found, for example, in [3].

exiting the collision area, as well as possibly having a negative velocity following the first such collision. In the simplified model, non-positive velocities are forbidden because they are equivalent to the particle travelling beyond the wall. In order to avoid such problems, if after the collision the particle has a negative velocity, we inject it back with the same modulus of velocity. Such a procedure is effected perfectly by use of a modulus function. Note that the velocity of the particle is reversed by the modulus function only if, after the collision, the particle remains travelling in the negative direction. The module function has no effect on the motion of the particle if it moves in the positive direction after the collision. We stress that this approximation is valid only for small values of ϵ. Moreover, it is no longer necessary to solve both of the functions $F(\phi_c)$ and $G(\phi_c)$. Incorporating these simplifications, the map can then be written as

$$T : \begin{cases} V_{n+1} = |V_n - 2\delta - 2\epsilon \sin(\phi_{n+1})| \\ \phi_{n+1} = \phi_n - \dfrac{1}{\delta} \ln\left[1 - \dfrac{2\delta}{V_n}\right] \mod 2\pi. \end{cases} \tag{10}$$

The phase ϕ_{n+1} is real only if $V_n > 2\delta$. If $V_n \leqslant 2\delta$, we can conclude that the particle does not have enough energy for a further collision. Therefore, the particle comes to rest. We then obtain the expression of the Jacobian matrix for this map (10), which takes the form

$$J_{\mathrm{sv}} = \begin{pmatrix} \frac{\partial \phi_{n+1}}{\partial \phi_n} & \frac{\partial \phi_{n+1}}{\partial V_n} \\ \frac{\partial V_{n+1}}{\partial \phi_n} & \frac{\partial V_{n+1}}{\partial V_n} \end{pmatrix}, \tag{11}$$

with coefficients given by

$$\frac{\partial \phi_{n+1}}{\partial \phi_n} = 1, \qquad \frac{\partial \phi_{n+1}}{\partial V_n} = -\frac{2}{V_n^2 - 2\delta V_n},$$

$$\frac{\partial V_{n+1}}{\partial \phi_n} = \mathrm{sign}[V_n - 2\delta - 2\epsilon \sin(\phi_{n+1})]\left[-2\epsilon \cos(\phi_{n+1}) \frac{\partial \phi_{n+1}}{\partial \phi_n}\right],$$

$$\frac{\partial V_{n+1}}{\partial V_n} = \mathrm{sign}[V_n - 2\delta - 2\epsilon \sin(\phi_{n+1})]\left[1 - 2\epsilon \cos(\phi_{n+1}) \frac{\partial \phi_{n+1}}{\partial V_n}\right],$$

where the function $\mathrm{sign}(u) = 1$ if $u > 0$ and $\mathrm{sign}(u) = -1$ if $u < 0$. The index 'sv' denotes the *simplified* version.

A careful investigation of the determinant of the Jacobian matrix (equation (11)) shows that $\det J_{\mathrm{sv}} = \mathrm{sign}[V_n - 2\delta - 2\epsilon \sin(\phi_{n+1})]$. This result tell us that, in contrast to the complete model, it is possible to observe regions of phase space where the area-preserving property is satisfied. As we will show, however, this result is not applicable throughout the whole of phase space.

3.1. Properties of the non-dissipative simplified FUM

Before considering the connections between the dissipative and non-dissipative cases, let us briefly discuss some properties of the simplified FUM (see footnote 3) without dissipation. Considering the case in which a particle bounces elastically between two rigid walls in the absence of a drag force and using the optimal variables, the map describing the dynamics of the simplified FUM is given by

$$\begin{cases} V_{n+1} = |V_n - 2\epsilon \sin(\phi_{n+1})| \\ \phi_{n+1} = \phi_n + \dfrac{2}{V_n} \mod 2\pi. \end{cases} \tag{12}$$

Table 1. Classification of periodic orbits of periods 1 and 2 for the simplified FUM in the absence of dissipation. We have used the letters H to classify a fixed point as hyperbolic, E as elliptic and finally P as parabolic.

Period	V	ϕ	ϵ	Type
1	$\frac{1}{j\pi}$, $j = 1, 2, 3\ldots$	0	All	H
1	$\frac{1}{j\pi}$, $j = 1, 2, 3\ldots$	π	$<\frac{1}{j^2\pi^2}$	E
1	$\frac{1}{j\pi}$, $j = 1, 2, 3\ldots$	π	$=\frac{1}{j^2\pi^2}$	P
1	$\frac{1}{j\pi}$, $j = 1, 2, 3\ldots$	π	$>\frac{1}{j^2\pi^2}$	H
2	$\frac{2}{j\pi}$, $j = 1, 3, 5\ldots$	$0, \pi$	$<\frac{2}{j^2\pi^2}$	E
2	$\frac{2}{j\pi}$, $j = 1, 3, 5\ldots$	$0, \pi$	$=\frac{2}{j^2\pi^2}$	P
2	$\frac{2}{j\pi}$, $j = 1, 3, 5\ldots$	$0, \pi$	$>\frac{2}{j^2\pi^2}$	H

The phase space for this system exhibits KAM islands surrounded by a chaotic sea that is limited by an invariant spanning curve in the low energy domain. For high energy, it basically shows a set of invariant spanning curves. As discussed in [44], the position of the lowest energy invariant spanning curve can be rescaled for different control parameters and connected to the standard map (SM) to appear for the same effective control parameter ($K_{\mathrm{FU}} \approx 0.97\ldots$) at which the SM undergoes a change from locally to globally stochastic behaviour[4]. Table 1 shows the classification of periodic orbits for the FUM.

3.2. Connection between the dissipative and non-dissipative cases

The dissipative model must go over into the non-dissipative one when the drag coefficient $\delta \to 0$. In this case, it is easy to see that the first equation of map (10) recovers the first equation of map (12), i.e.

$$V_{n+1} = \lim_{\delta\to 0} |V_n - 2\delta - 2\epsilon \sin(\phi_{n+1})|.$$

Considering the second equation of map (10), we obtain

$$\phi_{n+1} = \lim_{\delta\to 0}\left(\phi_n - \frac{1}{\delta}\ln\left[1 - \frac{2\delta}{V_n}\right]\right) = \phi_n + \frac{2}{V_n}. \tag{13}$$

It is also interesting to characterize how the fixed points of our dissipative model go over to the fixed points of the non-dissipative model. It is well known that the fixed points and periodic orbits are obtained by requiring that the conditions $\phi_{n+i} = \phi_n$ and $V_{n+i} = V_n$ are satisfied. The periodicity of the orbit is given by the label i, so $i = 1$ implies a period-one orbit, $i = 2$ gives a period-two orbit and so on. Applying the condition to obtain a period-one fixed point for both the equations of map (10), we obtain

$$V_{n+1} = V_n - 2\delta - 2\epsilon \sin(\phi_{n+1}) = V_n, \tag{14}$$

$$\phi_{n+1} = \phi_n - \frac{1}{\delta}\ln\left[1 - \frac{2\delta}{V_n}\right] = \phi_n. \tag{15}$$

Equation (14) yields

$$V_n = \frac{2\delta}{1 - \mathrm{e}^{-2\pi\delta i}} \qquad \text{with} \quad i = 1, 2, 3\ldots \tag{16}$$

[4] We have used the same notation as the original work [3] although, at that time, stochasticity was frequently referred as to chaotic behaviour. However, we emphasize that the transition is from locally to globally chaotic behaviour. In the FUM, we mean by *locally* that the chaotic behaviour is confined by two different invariant spanning curves.

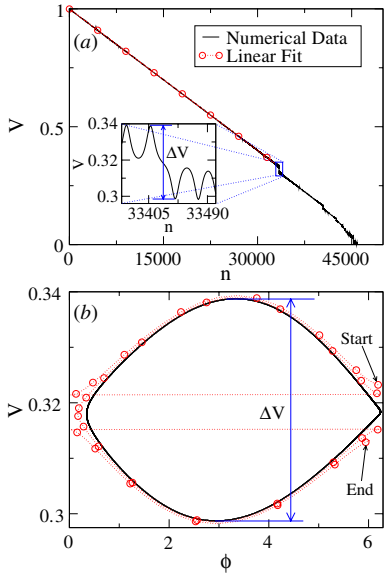

Figure 3. (*a*) The velocity $V(n)$ for $\epsilon = 1 \times 10^{-3}$, $\delta = 1 \times 10^{-5}$ for $V_0 = 1$ and $\phi_0 = 0$. The inset shows in more detail how V varies with n near to the KAM island of order $i = 1$. (*b*) Details of a trajectory passing near to a KAM island, plotting $V(n)$ as a function of the phase ϕ.

and then equation (15) gives us that

$$\phi_n = 2\pi - \arcsin(\delta/\epsilon), \tag{17}$$

$$\phi_n = \pi + \arcsin(\delta/\epsilon). \tag{18}$$

Equations (17) and (18) are both real for $\delta/\epsilon \leqslant 1$. We can use the coefficients of the Jacobian matrix (see equation (11)) and analyse the stability of the period-one fixed point. We then proceed as follows: (i) the fixed point given by equations (16) and (17) can be classified as hyperbolic for all values of the control parameters ϵ and δ with condition $\delta/\epsilon \leqslant 1$; (ii) for the fixed point given by equations (16) and (18) we define an auxiliary variable as

$$\epsilon^* = \frac{4\delta^2 \, \mathrm{e}^{-2\pi\delta i}}{\cos(\arcsin(\delta/\epsilon))[1 - \mathrm{e}^{-2\pi\delta i}]^2}, \tag{19}$$

and then use it to classify such a fixed point as (a) elliptic if $\epsilon < \epsilon^*$; (b) parabolic if $\epsilon = \epsilon^*$ and finally (c) hyperbolic if $\epsilon > \epsilon^*$.

3.3. Numerical results for the simplified dissipative FUM

We discuss in this section our numerical results for the simplified version of the model. Iterating the expression for the velocity given by the map (10), we again obtain the same equation (8) as for the complete model. It may thus be expected that, at high energy, the velocity of the particle decreases linearly on average, while oscillating sinusoidally as it decreases. Unlike the complete version, however, the stable KAM islands with invariant curves are observed. Such curves act effectively as barriers that do not allow the flux of particles to pass through them. Figure 3(*a*) shows the behaviour of the velocity as a function of iteration number. For high energy, the velocity of the particle decreases linearly, and a linear fit yields a coefficient

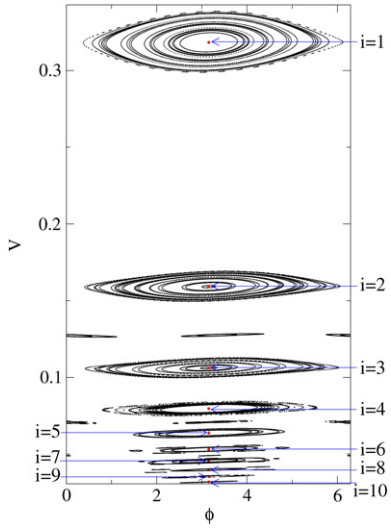

Figure 4. Stable regions in the phase space for the simplified dissipative model. The parameters used were $\epsilon = 1 \times 10^{-3}$ and $\delta = 1 \times 10^{-5}$. The period-one stable fixed points are represented by the dots and classified by the label i ($i = 1, 2, 3, \ldots, 10$), as shown.

of $-1.9990(7) \times 10^{-5}$ as predicted by equation (8). The expanded region of figure 3(*a*) illustrates the passage of the particle near to the invariant KAM curve delimiting the region related to the fixed point given by equations (16), with $i = 1$, and (18). Figure 3(*b*) shows a KAM curve (solid line) and the evolution of an initial condition near to the KAM curve (open circles connected by a dotted line as a guide to the eye). For visual clarity, we have only plotted every 4th point, i.e., between each two successive points connected by the dotted line there are another three that were not plotted. The gap observed in the inset of figure 3(*a*) has the same amplitude ΔV as observed in figure 3(*b*).

The stable regions for the simplified version of our model are shown in figure 4. As expected, the KAM curves surround an elliptic fixed point that is represented as a dot in figure 4. The parameters used in figure 4 were $\epsilon = 1 \times 10^{-3}$ and $\delta = 1 \times 10^{-5}$. For this combination of control parameters, the period-one elliptic fixed points are stable for $i \leqslant 10$. Moreover, outside these KAM curves, the particle behaves quite differently. We have shown that, in the regime of high energy, the velocity of the particle decreases linearly as iteration number increases. It passes around the stable KAM islands (see figure 3(*b*)) and then wanders chaotically in the low energy domain for a number of iterations. However, in the non-dissipative case, it is possible for the particle to have very low values of velocity within the so-called chaotic sea. It can assume low values in this version of the model too but, for the case where $V_n \leqslant 2\delta$, the particle has insufficient energy to return to the wall for its next kick, and it therefore comes to rest.

We now characterize this relaxation time for the simplified model in the low energy domain. To do so, we will evaluate the time evolution of an ensemble of different initial conditions in the regime of low energy. We will take different points uniformly distributed in the chaotic sea for the non-dissipative case as initial conditions and then study their asymptotic evolution in the dissipative case. However, as the drag force can cause some modifications to the form of the phase space, it is possible for some regions of the chaotic sea in the non-dissipative case to yield periodic or quasi-periodic behaviour in the dissipative version. If we then take an initial condition that leads to periodic or even quasi-periodic behaviour in

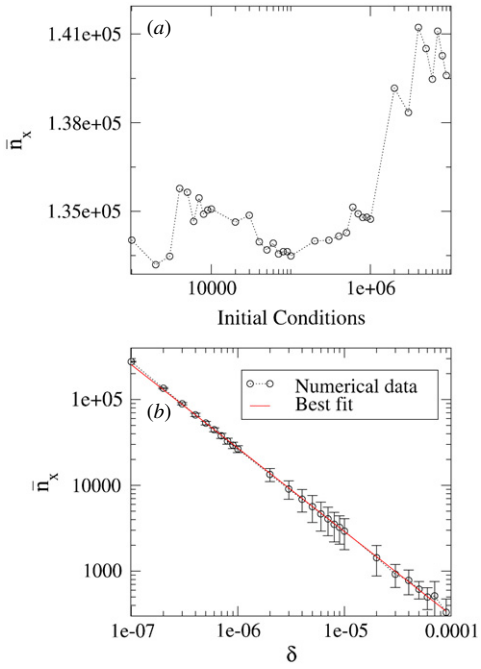

Figure 5. (*a*) Behaviour of the iteration number $\bar{n}_x$ as a function of the ensemble of initial conditions for the low energy region using $\delta = 2 \times 10^{-7}$ in the simplified version of the dissipative model. (*b*) The iteration number for the relaxation transient as a function of the parameter δ. The error bars represent the standard deviation for the ensemble of initial conditions used.

the dissipative model, it is disregarded and a different initial condition is then considered. Figure 5(*a*) shows the behaviour of the transient iteration number $\bar{n}_x$ (i.e., the number of iterations needed to bring the particle to rest) as a function of the number of initial conditions. Figure 5(*b*) illustrates the behaviour of the average transient $\bar{n}_x$ as a function of the strength of the drag coefficient. The error bars represent the standard deviation of the relaxation transient averaged over a set of 10^7 different initial conditions. These results allow us to describe the transient as

$$\bar{n}_x \propto \delta^{\mu}, \tag{20}$$

where a power-law fit gives us the exponent $\mu = -0.973(5) \approx -1$, which seems to be the same as that obtained in the complete model for a particle approaching the fixed point. Note however that, as discussed in the previous section for a fixed point convergence (see equation (9)), equation (20) diverges in the limit $\delta \to 0$. We can still conclude that in this limit of δ and as a consequence of the divergence of $\bar{n}_x$, the dynamics for such a region is in fact chaotic. It is also interesting to emphasize that all the invariant spanning curves are now stable in the limit $\delta \to 0$, a result that, in a sense, limits the size of the chaotic sea.

We now discuss why the area-preserving property is not applicable over the whole phase space of the simplified version of our model. We have shown that, for high energy, the velocity of the particle decreases linearly as the iteration number evolves. This behaviour brings the particle to the region where the chaotic transient is observed. However, as we have previously discussed, the particle experiencing a chaotic transient may assume very low velocity values. Moreover, the equations defining the map (see equation (10)) are restricted (defined for real

numbers) to the condition $V_n > 2\delta$. Thus, if the particle acquires a velocity $V_n \leqslant 2\delta$, the phase ϕ_{n+1} is not defined as a real number, corresponding to the particle having insufficient energy for a further collision. As an immediate consequence, the dynamics of the system is over. Note however that the condition $V_n \leqslant 2\delta$ breaks down the property of area preservation, since the map is undefined for that range of V_n. Moreover, for the stable KAM islands that surround the elliptic fixed points (see figure 4), the particle does not assume these velocities $V_n \leqslant 2\delta$. Once within this region (KAM islands) for which the phase ϕ is real for all values of the velocity, area preservation applies.

Let us now discuss this apparent paradox. The interested reader will be able to find a specific example and a more complete discussion in [53]. First, we emphasize that the definition of a *dissipative* system is not quite so clear as it seems at first sight. One might say that 'dissipative' implies that the phase space volume is not conserved under time evolution. Alternatively, one might say that 'dissipative' denotes that friction is present. In our model however we have, by construction, a friction force present but, counter-intuitively, the determinant of the Jacobian matrix is unity. Why does this result not contradict the statement that there are no attractors in the model studied? The answer is related to the Poincaré recurrence theorem. This theorem, which is also a consequence of the Liouville's theorem, states that for a *bounded* phase space, almost all trajectories eventually return arbitrarily close to where they started. It is interesting to note that this result is true regardless of whether the trajectory under consideration is regular or chaotic. Our results for high energy show convincingly that the particle velocity decreases linearly as the iteration number increases. Eventually, the particle enters the corresponding region of the chaotic sea (for the non-dissipative case) and we observe that $V \to 0$. Thus, it is easy to conclude that the time for the next collision $t \to \infty$, so that the phase space is unbounded. We also comment that in the present dissipative version there is no mechanism for accelerating the particle to high energy (say higher than $V_c \cong 2\sqrt{\epsilon/0.97\ldots}$, see [44]). Thus, the Poincaré recurrence argument is not satisfied.

Finally, we point out that the coexistence of conservative and dissipative behaviour has also been observed in a laser [54], where it was attributed to the occurrence of a symmetry-breaking bifurcation, leading to the appearance of a structurally stable homoclinic cycle.

Before presenting our conclusions, we first comment on the comparisons of our results with previous and well-known results in the literature. It is important to note that the kind of dissipation used in the present paper acts as a bouncing ball, continuously bouncing along. Such a dissipative force is contrary to the inelastic collisions that modify the ball's velocity only at the instant of the impact. Despite both kinds of damping often occuring in nature, they have profound and different consequences in the dynamics of the bouncing ball model. As an example, in [38, 39] and considering inelastic collisions, Tsang and Lieberman considered the simplified FUM with inelastic impacts. They present evidence of contraction on the phase space and, in particular, they have observed the presence of a strange attractor. Recently, we have used a very similar version of the dissipative model [41], confirmed the property of area contraction and in addition characterized a boundary crisis. A closely related model, the gravitational bouncer model, was also considered under inelastic collisions. For example, in [33] Holmes discusses the appearances of horseshoes in the inelastic bouncer and gave an illustration of a homoclinic orbit in such a model. Four years later, Everson [35] presents and discusses with many numerical simulations the appearance of period doubling cascade again, the damping bouncer model. Period doubling cascade was also observed in [34] for the completely inelastic collisions. The presence of frictional force however was considered by Luna-Acosta [37] and Naylor, Sanchéz and Swift [36] in the bouncer model. They too observed period doubling cascades and in particular Luna-Acosta [37] has achieved

analytically dimensional reduction for the limit of high dissipation. It is worth stressing that the above models do not present singularities in the mapping expressions as they appear in the equations of our dissipative version. They appear as a consequence of the particle's energy being entirely dissipated by the damping force.

In the bouncer model, after the particle leaves the moving wall (the same procedure might be applied in the simplified version), there is always a returning mechanism that brings the particle for a next collision. Such a mechanism works even in the regime of high frictional coefficient and it depends basically on the strength of the gravitational field. For inelastic collisions, with the inelasticity settled in the moving wall, the completely inelastic case yields the phenomenon of the locking regime [32]. In our model, however, depending on the region of the phase space for both the complete and simplified versions, the particle reaches the limit of $V \to 0$ and then the returning mechanism stops working since collisions no longer happen. Another point that must be emphasized is related to the canonical variables of the model (see [3], chapter 3, section 3.4a). On the complete version, the extended phase space is $(V, X, -E, t)$ and the canonical pairs are $(-E, t)$ and (V, X). Thus, the reason for not observing the determinant of the Jacobian matrix being unity for $\gamma \to 0$ in the complete model is that the variables chosen on the description of the problem are not canonically conjugate. On the simplified version however the canonical pair is (V, ϕ), thus such a pair of variables leads to the recovery of the determinant of the Jacobian matrix to unity. Despite the phase space of the model appearing to be very similar on the conservative case, the introduction of frictional force proportional to the particle's velocity drastically affects the regions of the chaotic sea and invariant spanning curves, consequently destroying them. However the KAM islands survive such a perturbation in the simplified version and turn them into attracting sinks on the complete version. Moreover and as a final comment, even for different versions of the model, our results for the transient time on the corresponding region of the chaotic sea for the non-dissipative case, i.e. the number of iterations needed to bring the particle to rest, seem to be described by a power law with the same exponent.

4. Conclusions

We have studied the FUM in the presence of a drag force, described by use of a two-dimensional map obtained via the solution of differential equations. The complete version of the model is area contracting and we have characterized the time evolution of the velocity in the regime of high energy, where it seems to decrease linearly as the iteration number increases. In the regime of low energy, the particle may be captured by an attracting region or can come to rest once all its energy have been dissipated by the drag force. If the particle is captured by an attracting region, it approaches the fixed point exponentially as the iteration number increases. We show that the simplified model possesses some regions in its phase space where the property of area preservation is observed, exhibiting the stable KAM islands. For high energy, the behaviour of the velocity seems to be the same as in the complete model. However, in the low energy regime, and outside the KAM islands, the particle relaxes via a chaotic transient that depends on the strength of the drag coefficient.

Finally, we comment on the relationship between the simplified and full FUMs. It is well known that the simplified version of the non-dissipative FUM yields qualitatively very similar results to those obtained from the complete model. We have shown in this paper, however, that in the presence of a drag force the simplified model yields results that are entirely different from those of the complete version within certain regions of the phase space. In particular, the simplified model possesses regions in its phase space where the property of area preservation is observed, a result that does not arise in the complete version.

Acknowledgments

EDL is grateful to CNPq and FAPESP, Brazilian agencies; PVEMcC gratefully acknowledges support from the Engineering and Physical Sciences Research Council (UK).

Appendix

Solution of equation (1) for the given initial conditions and redefining the time as $t \to t - t_n$, for $t \geqslant t_n$, yield

$$v_{\mathrm{p}}(t) = v_n \, \mathrm{e}^{-\eta t}, \tag{A.1}$$

where we have defined $\eta = \eta'/m$. Considering now $v_{\mathrm{p}}(t) = \mathrm{d}x_{\mathrm{p}}(t)/\mathrm{d}t$ and using both the initial conditions and equation (A.1), we obtain the position of the particle as

$$x_{\mathrm{p}}(t) = \varepsilon \cos(\omega t_n) + \frac{v_n}{\eta}[1 - \mathrm{e}^{-\eta t}]. \tag{A.2}$$

Let us now discuss the different possibilities that may arise in our model. Depending on both the initial velocity v_n and initial time t_n, they are as follows:

(a) The particle suffers another collision with the moving wall before exiting the collision area. Such a collision will be referred to as a *successive collision*.
(b) The particle exits the collision area without suffering a further collision.

The collision area is defined as the interval $x \in [-\varepsilon, \varepsilon]$ within which it is possible for the particle to collide with the time-varying wall.

In case (a), the condition for observing successive collisions is obtained from $x_{\mathrm{p}}(t) = x_{\mathrm{w}}(t)$ for $x_{\mathrm{p}}(t) \leqslant \varepsilon$. This leads to the transcendental equation

$$g(t_c) = \varepsilon \cos[\omega(t_n + t_c)] - \varepsilon \cos(\omega t_n) - \frac{v_n}{\eta}[1 - \mathrm{e}^{-\eta t_c}], \tag{A.3}$$

where t_c is the smallest root of equation (A.3) for $t_c \in (0, 2\pi/\omega]$. The same discussion of the redefined time also holds here for t_c. Note however that the time $t_c = 0$ is excluded because it is a fixed point of $g(t_c) = 0$. The velocity immediately after the impact with the moving wall is obtained from the requirement that energy and momentum in the frame of reference of the moving wall are conserved. This procedure is needed because, at the moment of impact, the moving wall can be considered to be instantaneously at rest. The new velocity is given by $v_{n+1} = -v_n \, \mathrm{e}^{-\eta t_c} + 2v_{\mathrm{w}}(t_{n+1})$ where $v_{\mathrm{w}}(t) = \mathrm{d}x_{\mathrm{w}}(t)/\mathrm{d}t = -\varepsilon\omega \sin(\omega t)$. For such a successive collision, the map is then written as

$$T_m : \begin{cases} v_{n+1} = -v_n \, \mathrm{e}^{-\eta t_c} - 2\varepsilon\omega \sin(\omega t_{n+1}) \\ t_{n+1} = t_n + t_c. \end{cases} \tag{A.4}$$

The index 'm' denotes that the mapping describes *multiple* (collisions) with the moving wall. If $g(t_c)$ does not have a solution for $t_c \in (0, 2\pi/\omega]$ we may conclude that the particle leaves the collision area without suffering a further collision, so that case (b) applies. Either of two different things may then occur: (b_1) the drag force dissipates part of the energy of the particle and, after it hits the fixed wall and is reflected backwards, it suffers another collision with the moving wall or (b_2) the drag force dissipates all the energy of the particle. We now obtain the equation for case (b_1). Note, however, that case (b_2) (dissipation of all the particle's energy) is completely encompassed by the equations obtained for (b_1). After leaving the collision area, the particle travels to the right, i.e. towards the fixed wall located at $x = l$, suffers an elastic collision and is reflected back towards the moving wall. During this part of its trajectory, both the velocity and position of the particle are described by equations (A.1) and (A.2). We

thus need to evaluate the velocity of the particle and corresponding time immediately before it re-enters the collision area. The time spent in this part of its trajectory is easily obtained by evaluation of equation (A.2) taking into consideration that $x_p = 2l - \varepsilon$. We then find that

$$t_T = -\frac{1}{\eta}\ln\left[1 - \frac{\eta}{v_n}[2l - \varepsilon - \varepsilon\cos(\omega t_n)]\right]. \tag{A.5}$$

Equation (A.5) is real only if $v_n > \eta[2l - \varepsilon - \varepsilon\cos(\omega t_n)]$. For the condition $v_n \leqslant \eta[2l - \varepsilon - \varepsilon\cos(\omega t_n)]$ we can conclude that case (b_2) occurs, i.e. the drag force has already dissipated all of the energy of the particle. Consequently, the particle has come to rest. If the velocity of the particle satisfies equation (A.5), then it re-enters the collision area and will certainly suffer another collision with the moving wall. Its velocity for $t = t_T$ is obtained from equation (A.1) taking the negative direction because the particle has been reflected by the fixed wall located at $x = l$. It is given by

$$v_{\rm p}(t_T) = -v_n + 2\eta l - \eta\varepsilon[1 + \cos(\omega t_n)]. \tag{A.6}$$

The time at which the particle suffers a collision with the moving wall is obtained from condition $x_{\rm p}(t_n + t_T + t) = x_{\rm w}(t_n + t_T + t)$. It then leads to the following transcendental equation:

$$f(t_c) = \varepsilon\cos[\omega(t_n + t_T + t_c)] - \varepsilon - (1 - {\rm e}^{-\eta t_c})\left[\frac{v_{\rm p}(t_T)}{\eta}\right], \tag{A.7}$$

where t_c is the smallest solution of $f(t_c)$ for $t_c \in [0, 2\pi/\omega]$. The map is then written as

$$T_s : \begin{cases} v_{n+1} = -v_{\rm p}(t_T)\,{\rm e}^{-\eta t_c} - 2\varepsilon\omega\sin(\omega t_{n+1}) \\ t_{n+1} = t_n + t_T + t_c. \end{cases} \tag{A.8}$$

The index 's' denotes single collisions with the time-varying wall.

References

[1] Fermi E 1949 *Phys. Rev.* **75** 1169
[2] Walker G H and Ford J 1969 *Phys. Rev.* **188** 416
[3] Lichtenberg A J and Lieberman M A 1992 *Regular and Chaotic Dynamics (Appl. Math. Sci.* vol 38*)* (New York: Springer)
[4] Lieberman M A and Lichtenberg A J 1972 *Phys. Rev.* A **5** 1852
[5] Kruger T, Pustylnikov L D and Troubetzkoy S E 1995 *Nonlinearity* **8** 397
[6] Wiesenfeld K and Tufillaro N B 1987 *Physica* D **26** 321
[7] Ulam S 1961 *Proc. 4th Berkeley Symposium on Math, Statistics and Probability* vol 3 (Berkeley, CA: University of California Press) p 315
[8] Pustylnikov L D 1977 *Trudy Moskov. Mat. Obsc.* **34** 1
Pustylnikov L D 1983 *Theor. Math. Phys.* **57** 1035 (Engl. Transl.)
[9] Lichtenberg A J, Lieberman M A and Cohen R H 1980 *Physica* D **1** 291
[10] Leonel E D and McClintock P V E 2005 *J. Phys. A: Math. Gen.* **38** 823
[11] Karner G 1994 *J. Stat. Phys.* **77** 867
[12] Dembinski S T, Makowski A J and Peplowski P 1983 *Phys. Rev. Lett.* **70** 1093
[13] José J V and Cordery R 1986 *Phys. Rev. Lett.* **56** 290
[14] Seba P 1990 *Phys. Rev.* A **41** 2306
[15] Jain S R 1993 *Phys. Rev. Lett.* **70** 3553
[16] Kowalik Z J, Franaszek M and Pieranski P 1988 *Phys. Rev.* A **37** 4016
[17] Warr S, Cooke W, Ball R C and Huntley J M 1996 *Physica* A **231** 551
[18] Warr S and Huntley J M 1995 *Phys. Rev.* E **52** 5596
[19] Leonel E D and McClintock P V E 2005 *Chaos* **15** 033701
[20] Mateos J L 1999 *Phys. Lett.* A **256** 113
[21] Luna-Acosta G A, Orellana-Rivadeneyra G, Mendoza-Galván A and Jung C 2001 *Chaos Solitons Fractals* **12** 349

[22] Leonel E D and da Silva J K L 2003 *Physica* A **323** 181
[23] Leonel E D and McClintock P V E 2004 *Phys. Rev.* E **70** 016214
[24] Leonel E D and McClintock P V E 2004 *J. Phys. A: Math. Gen.* **37** 8949
[25] Berry M V 1981 *Eur. J. Phys.* **2** 91
[26] Saitô N, Hirooka H, Ford J, Vivaldi F and Walker G H 1982 *Physica* D **5** 273
[27] Robnik M and Berry M V 1985 *J. Phys. A: Math. Gen.* **18** 1361
[28] Egydio de Carvalho R 1997 *Phys. Rev.* E **55** 3781
[29] Loskutov A, Ryabov A B and Akinshin L G 2000 *J. Phys. A: Math. Gen.* **33** 7973
[30] Egydio de Carvalho R, de Sousa F C and Leonel E D 2006 *J. Phys. A: Math. Gen.* **39** 3561
[31] Egydio de Carvalho R, Sousa F C and Leonel E D 2006 *Phys. Rev.* E **73** 066229
[32] Mehta A and Luck J M 1990 *Phys. Rev. Lett.* **65** 393
[33] Holmes P J 1982 *J. Sound Vibr.* **84** 173
[34] Luck J M and Mehta A 1993 *Phys. Rev.* E **48** 3988
[35] Everson R M 1986 *Physica* D **19** 355
[36] Naylor M A, Sánchez P and Swift M R 2002 *Phys. Rev.* E **66** 57201
[37] Luna-Acosta G A 1990 *Phys. Rev.* A **42** 7155
[38] Tsang K Y and Lieberman M A 1986 *Physica* D **21** 401
[39] Lieberman M A and Tsang K Y 1985 *Phys. Rev. Lett.* **5** 908
[40] Lichtenberg A J and Lieberman M A 1992 *Regular and Chaotic Dynamics (Appl. Math. Sci.* vol 38*)* (New York: Springer) ch 8, section 8.1a
[41] Leonel E D and McClintock P V E 2005 *J. Phys. A: Math. Gen.* **38** L425
[42] Tsang K Y and Ngai K L 1997 *Phys. Rev.* E **56** R17
[43] Leonel E D and McClintock P V E 2006 *Phys. Rev.* E **73** 066223
[44] Leonel E D, da Silva J K L and Kamphorst S O 2004 *Physica* A **331** 435
[45] Kamphorst S O and de Carvalho S P 1999 *Nonlinearity* **12** 617
[46] Leonel E D, McClintock P V E and da Silva J K L 2004 *Phys. Rev. Lett.* **93** 014101
[47] Barabási A-L and Stanley H E 1985 *Fractal Concepts in Surface Growth* (Cambridge: Cambridge University Press)
[48] Ladeira D G and da Silva J K L 2006 *Phys. Rev.* E **73** 026201
[49] da Silva J K L, Ladeira D G, Leonel E D, McClintock P V E and Kamphorst S O 2006 *Braz. J. Phys.* **36** 700
[50] Luna-Acosta G A, Na K, Reichl L E and Krokhin A 1996 *Phys. Rev.* E **53** 3271
[51] Luna-Acosta G A, Méndez-Bermúdez J A and Izrailev F M 2001 *Phys. Rev.* E **64** 36206
[52] Lichtenberg A J and Lieberman M A 1992 *Regular and Chaotic Dynamics (Appl. Math. Sci.* vol 38*)* (New York: Springer) ch 6, section 6.1b
[53] Sussman G J, Wisdom J and Mayer M E 2001 *Structure and Interpretation of Classical Mechanics* (Cambridge, MA: MIT Press)
[54] Politi A, Oppo G L and Badii R 1986 *Phys. Rev.* A **33** 4055